Life Sciences 90 (2012) 934–943

Contents lists available at SciVerse ScienceDirect

Life Sciences

journal homepage: www.elsevier.com/locate/lifescie

The modulation of hepatic adenosine triphosphate and inflammation by eicosapentaenoic acid during severe fibrotic progression in the SHRSP5/Dmcr rat model

Xiaofang Jia [a], Hisao Naito [a], Husna Yetti [a], Hazuki Tamada [a,b], Kazuya Kitamori [a,b], Yumi Hayashi [a], Nozomi Yamagishi [a], Dong Wang [a], Yukie Yanagiba [a], Yuki Ito [c], Juncai Wang [a], Naoki Tanaka [d], Katsumi Ikeda [e], Yukio Yamori [f], Tamie Nakajima [a,*]

[a] Department of Occupational and Environmental Health, Nagoya University Graduate School of Medicine, Nagoya, Japan
[b] College of Human life and Environment, Kinjo Gakuin University, Nagoya, Japan
[c] Department of Occupational and Environmental Health, Nagoya City University Graduate School of Medical Sciences, Nagoya, Japan
[d] Laboratory of Metabolism, National Cancer Institute, National Institutes of Health, Bethesda, USA
[e] School of Pharmacy and Pharmaceutical Sciences, Mukogawa Women's University, Nishinomiya, Japan
[f] Institute for World Health Development, Mukogawa Women's University, Nishinomiya, Japan

ARTICLE INFO

Article history:
Received 13 December 2011
Accepted 21 April 2012

Keywords:
Eicosapentaenoic acid
High fat-cholesterol diet
Fibrotic steatohepatitis
Nuclear factor-κB
Fatty acid β-oxidation
Adenosine triphosphate

ABSTRACT

Aims: Eicosapentaenoic acid (EPA) can ameliorate certain liver lesions involved in non-alcoholic steatohepatitis (NASH). A previous study has found that stroke-prone spontaneously hypertensive 5/Dmcr (SHRSP5/Dmcr) rats fed a high fat-cholesterol (HFC) diet developed fibrotic steatohepatitis with histological similarities to NASH. This study evaluated the potential effects and mechanisms of action of EPA supplementation using this rodent model.
Main methods: Male rats were randomly assigned to groups that were fed with either the stroke-prone (SP) diet or HFC diet with or without EPA for 2, 8 and 14 weeks, respectively. The liver histopathology, biochemical features, mRNA and protein levels, and nuclear factor-κB (NF-κB) DNA binding activity were determined.
Key findings: The SP diet-fed rats presented normal livers. Conversely, the HFC diet-fed rats developed microvesicular/macrovesicular steatosis, inflammation, ballooning degeneration and severe fibrosis. At 2 weeks, the administration of EPA inhibited hepatic inflammatory recruitment by blocking the phosphorylation of inhibitor of κB-α (IκBα), which antagonizes the NF-κB activation pathway. The dietary supplementation of EPA for 8 weeks ameliorated hepatic triglyceride accumulation and macrovesicular steatosis by inhibiting the HFC diet-induced decrease in the protein levels of enzymes involved in fatty acid β-oxidation including carnitine palmitoyltransferase 1, very long chain acyl-CoA dehydrogenase and peroxisomal bifunctional protein. Although the administration of EPA elicited no histologically detectable effects on severe fibrosis at 14 weeks, it restored an HFC diet-induced decline in hepatic adenosine triphosphate (ATP) levels and suppressed ballooning degeneration, suggesting that EPA may inhibit HFC diet-induced ATP loss and cell death.
Significance: Initial amelioration of the inflammation and steatosis in the rats after EPA supplementation indicates a possibility to treat steatohepatitis. Additionally, this study provides new insights into the roles of EPA in hepatic ATP depletion and subsequent hepatocellular injury during severe fibrosis.

Introduction

Non-alcoholic steatohepatitis (NASH), a more severe and progressive form of non-alcoholic fatty liver disease (NAFLD), is characterized by steatosis, inflammation and fibrosis, which can progress to cirrhosis and hepatocellular carcinoma (de Alwis and Day, 2008). NASH is prevalent among individuals with obesity and diabetes, as well as among non-obese and non-diabetic populations, affecting 2–3% of the general adult population (de Alwis and Day, 2008; Neuschwander-Tetri and Caldwell, 2003). The increasing prevalence of NASH appears to be related to a Westernized lifestyle, characterized by a lack of physical exercise and increased consumption of hypercaloric food, cholesterol and saturated fat (Cortez-Pinto and Machado, 2008; Enjoji and Nakamuta, 2010). Such a lifestyle contributes to the accumulation of visceral fat and the development of insulin resistance, hypertriglyceridemia and NAFLD. As such, NASH and its treatment and management have become the subject of intense investigation. However, the exact treatment strategy for NASH remains poorly established.

* Corresponding author at: Department of Occupational and Environmental Health, Nagoya University Graduate School of Medicine, 65 Tsurumai-cho, Showa-ku, Nagoya 466-8550, Japan. Tel.: +81 52 744 2122; fax: +81 52 744 2126.
E-mail address: tnasu23@med.nagoya-u.ac.jp (T. Nakajima).

0024-3205/$ – see front matter © 2012 Elsevier Inc. All rights reserved.
doi:10.1016/j.lfs.2012.04.029

Eicosapentaenoic acid (EPA) is one of the principal components of n-3 polyunsaturated fatty acid (PUFA) and has been used as a treatment for hyperlipidemia (Yokoyama et al., 2007). Investigators have speculated that EPA might be a promising therapy to prevent or ameliorate NASH based on its attenuation of all major histopathological features in NASH patients (Tanaka et al., 2008). In rodents, EPA was found to decrease de novo lipogenesis (Ishii et al., 2009; Kajikawa et al., 2009a, 2009b; Tanaka et al., 2010) and to induce fatty acid oxidation (Ishii et al., 2009), thereby ameliorating steatosis. EPA also decreased oxidative stress in the liver, consequently alleviating inflammation (Ishii et al., 2009; Kajikawa et al., 2009b, 2010). Furthermore, EPA attenuated the progression of hepatic fibrosis (Kajikawa et al., 2009b, 2010, 2011). However, the precise efficacy of EPA supplementation under various conditions must still be confirmed. The rodent dietary models used for evaluating the efficacy of EPA treatments have been limited, where EPA was either applied for a short treatment period in mice with minimal liver lesions (Kajikawa et al., 2009a, 2009b; Tanaka et al., 2010) or for a long treatment period (20 weeks) in rats until fibrogenesis was detected (Kajikawa et al., 2010, 2011). To date, no single animal model displaying the range of histopathological and pathophysiological features of human NASH has been developed. We recently used a high fat-cholesterol (HFC) diet to induce steatohepatitis, but not obesity or diabetes, in stroke-prone spontaneously hypertensive 5/Dmcr (SHRSP5/Dmcr) rats (Kitamori et al., in press). This model appeared to be a physiological dietary model of NASH without the obesity or insulin resistance observed in the general population. Moreover, compared to previous models, the liver pathology indicated steatohepatitis with hepatocellular ballooning and severe chicken-wire fibrosis (even cirrhosis in some cases), which are essential histological features that define human NASH (Kajikawa et al., 2009a, 2009b; Tanaka et al., 2010).

Overall, our model exhibited the disease progression and pathological features of NASH without the obesity and the insulin resistance due to HFC diet feeding over a 14-week period and could be used for the testing of the potency of therapeutic agents against liver lesions. Therefore, using this rodent model, we investigated the therapeutic functions and underlying mechanisms of EPA.

Materials and methods

Diets

Stroke-prone (SP: 20.8% crude protein, 4.8% crude lipid, 3.2% crude fiber, 5.0% crude ash, 8.0% moisture, and 58.2% carbohydrate) and high fat-cholesterol (HFC: a mixture of 68% SP diet, 25% palm oil, 5% cholesterol and 2% cholic acid) diets were obtained from Funabashi Farm (Chiba, Japan). The EPA was a kind gift from Mochida Pharmacy (Tokyo, Japan). The EPA-containing HFC diet was manually prepared every two days.

Animals

All of the animal experiments were conducted in compliance with the Guidelines for Animal Experiments of the Kinjo Gakuin University Animal Center. The male SHRSP5/Dmcr rats were obtained by mating males and females of the SHRSP5/Dmcr strain with high cholesterol levels (initially and kindly given by Y. Yamori, Emeritus Professor of Kyoto University) as previously described (Kitamori et al., in press). All of the rats were housed in a temperature- and light-controlled environment (23 ± 2 °C, 55 ± 5% humidity, 12-h light/dark cycle) with free access to the control chow (SP diet) and tap water.

Experimental protocols

At 10 weeks of age, the male offspring were randomly divided into 9 groups of 6 rats each and fed with SP or HFC diet with or without EPA (1 mg/g body weight/day) for 2, 8 and 14 weeks, respectively. No differences in energy intake were observed between the HFC diet-fed and EPA-treated groups. After 18–20 h of fasting from the last feeding of each group, the rats were weighed, anesthetized by pentobarbital (70 mg/kg) and sacrificed. Blood samples were collected, and the livers were removed and weighed. A portion of each liver was fixed with 10% buffered formalin for histopathological analysis, immersed in RNAlater solution or quickly stored at −80 °C until use. The serum was prepared by centrifugation of the blood samples at 3500 *g* for 10 min and stored at −80 °C until use.

Histopathology

The formalin-fixed liver tissues were subjected to hematoxylin and eosin (H&E) staining and modified Elastic Van Gieson (EVG) staining using Sirius red stain. The histopathological changes were assessed using a DMD108 microscope (Leica, Wetzlar, Germany) and scored for H&E staining according to the criteria proposed by Kleiner et al. (2005): (1) steatosis: 0, none; 1, mild (5–33% of parenchymal involvement by steatosis); 2, moderate (33–66%); 3, severe (>66%); (2) lobular inflammation: 0, none; 1, mild (<2 foci per 200× field); 2, moderate (2–4 foci); 3, severe (>4 foci); (3) hepatocyte ballooning: 0, none; 1, few ballooned cells; 2, many cells/prominent ballooning; and (4) macrovesicular steatosis: the same as that of steatosis. The NAFLD activity score (NAS) was defined as the unweighted sum of steatosis, lobular inflammation, and hepatocyte ballooning, with a maximum score of 8. The fibrotic area of EVG-stained sections was evaluated using BZ-9000 and Dynamic cell counter (Keyence, Osaka, Japan).

Biochemical assays of serum and liver extracts

The levels of serum triglyceride (TG), γ-glutamyl transpeptidase (γ-GTP), aspartate aminotransferase (AST) and alanine aminotransferase (ALT) were determined by S.R.L. Inc. (Tokyo, Japan). Commercial kits were used for the measurement of serum interleukin-6 (IL-6), tumor necrosis factor-α (TNF-α) (R&D Systems Inc., Minneapolis, MN), and adiponectin (Otsuka Pharmaceuticals, Tokyo, Japan). The hepatic lipid was extracted as described by Folch et al. (1957). The hepatic TG content was measured using the TG-IE kit (Wako, Osaka, Japan). All of the experiments were repeated at least two times.

Measurement of intracellular adenosine triphosphate (ATP) levels

The levels of intracellular ATP were measured using the "Cellno" ATP Assay reagent (Toyo B-Net Co., Ltd, Tokyo, Japan). Briefly, the liver tissues were lysed with 0.25 M sucrose in 10 mM HEPES buffer. 100 μl of each diluted sample or standard was transferred into a disposable cuvette and mixed with 100 μl of luciferase reagent. After mixing, the light emitted was measured and integrated for 10 s using an AP-2200CP (ATTO, Tokyo, Japan). The ATP concentrations were calculated from the linear portion of a standard curve and expressed as 10^{-6} mmol/g liver.

Real-time quantitative PCR

The total RNA was isolated from whole livers using the RNeasy Mini Kit (QIAGEN, Tokyo, Japan). Real-time PCR analysis was performed as described previously (Ramdhan et al., 2010). We normalized all of the mRNA levels to glyceraldehyde-3-phosphate dehydrogenase (GAPDH) mRNA in the same preparation. The primer sequences are listed in the Supplementary Table 1.

Western blot analysis

Sections of liver were homogenized with 3 volumes of 0.25 M sucrose-10 mM phosphate buffer (pH 7.4). The cytosolic fractions

were prepared at 4 °C by differential centrifugation. The nuclear fractions were extracted from portions of frozen liver using the CelLytic™ NuCLEAR™ Extraction Kit (SIGMA, Tokyo, Japan). The samples were subjected to 10% sodium dodecyl sulfate-polyacrylamide gel electrophoresis as described previously (Ramdhan et al., 2010). The membranes were incubated with the following antibodies: SREBP-1c, PPARα, DGAT2, NF-κB p50 and NF-κB p65 (Santa Cruz Biotechnology, Santa Cruz, CA); FAS and CPT1 (GeneTex, San Antonio, TX); MCP-1 (Biovision Inc., San Francisco, CA); SCD1 (Abnova, Taipei, Taiwan); IKKα, IKKβ, phospho-IKKα/β, IκBα, phospho-IκB-α, ERK, phospho-ERK, JNK and phospho-JNK (Cell Signaling Technology, Beverly, Massachusetts); and VLCAD and PH (the kind gift of Professor Aoyama of Shinshu University, Japan). Immunoblotting with GAPDH (Santa Cruz Biotechnology, Santa Cruz, CA) and Lamin-B1 (MBL, Nagoya, Japan) antibodies was performed for loading controls. For the detection of specific proteins, the 1-Step™ NBT/BCIP (Pierce Biotechnology, Rockford, IL, USA) or ECL Western Blotting Detection Reagent (GE Healthcare, Buckinghamshire, UK) was used.

Nuclear factor-κB (NF-κB) activation assay

The NF-κB p65 DNA binding activity was assessed by the TransAM™ NF-κB Kit (Active Motif, Carlsbad, CA) using nuclear protein according to the manufacturer's protocols.

Statistical analysis

The values were expressed as the mean ± the standard deviation. Apart from the histopathological scoring results analyzed by the Mann–Whitney *U* test between SP and HFC, HFC and EPA groups, the other results were tested using Student's *t*-test. If the variance was heterogeneous, logarithm or square root transformation was performed before the analysis. All of the analyses were performed using the SPSS 17.0 program. *P* values less than 0.05 were considered statistically significant.

Results

The effects of EPA on body weight, liver weight and relative liver weight

The rats fed with HFC diet with or without EPA developed lower body weights and higher absolute and relative liver weights than the SP-fed control rats. Unexpectedly, the EPA-treated rats exhibited decreased body weight at 2 weeks and increased absolute and relative liver weights at 14 weeks compared to rats fed with HFC diets alone (Table 1).

The effects of EPA on serum or liver parameters

As shown in Table 1, HFC diet-fed rats exhibited higher serum levels of AST, ALT, γ-GTP and IL-6, indicating the presence of hepatic injuries, whereas the EPA treatment resulted in a marked decrease in the levels of γ-GTP and IL-6 at 8 weeks. The HFC diet-fed rats developed persistently increased levels of pro-inflammatory TNF-α and gradually decreased levels of the anti-inflammatory cytokine, adiponectin. Conversely, the EPA supplementation substantially reduced TNF-α and elevated adiponectin levels at 2 and 8 weeks, respectively, followed by lower TNF-α/adiponectin. Neither the HFC diet nor the supplementation of EPA changed the serum levels of insulin or glucose (data not shown). To clarify the effects of EPA on the accumulation of fat in the liver, the hepatic and serum TG contents were measured. The HFC diet induced higher hepatic TG levels at each period compared to the control diet, whereas the EPA supplementation for 8 weeks significantly decreased TG levels from 36 ± 12 to 18 ± 7 mg/g of liver tissue. Moreover, compared to the HFC diet-fed group, the EPA remarkably decreased the serum TG levels at 2 weeks. The hepatic and serum total cholesterol levels were also determined and will be reported elsewhere (in preparation).

The effects of EPA on histopathology

The control rats exhibited normal livers throughout the entire study (Fig. 1A and B), although slight inflammatory infiltration was occasionally observed. At 2 weeks, the H&E staining revealed that the HFC diet-fed rats exhibited mild steatosis with foci of inflammatory infiltration, which progressed to extensive steatosis with large vacuoles, accompanied by inflammation and ballooning degeneration at 8 and 14 weeks (Fig. 1A). The EPA supplementation for 2 weeks appeared to reduce the inflammatory infiltration, and to improve the macrovesicular steatosis at 8 weeks, as well as the hepatocyte ballooning at 14 weeks. Interestingly, more hepatocytes with a bright pink color and natural nuclei existed in the EPA group in the last stage. Conversely, more hepatocytes with a dull pink color were observed in the HFC group. Some of these hepatocytes experienced pyknosis and karyorrhexis; their intercellular boundaries became more obscure. These differences indicated that the more active cells might have persisted in rats treated with EPA, particularly at 14 weeks.

According to the mean scores (Table 2), rats fed with the HFC diet progressively developed steatosis and even macrovesicular steatosis, lobular inflammation and ballooning degeneration compared to the rats fed the control diet. At 2 weeks, the rats treated with EPA exhibited significant improvement of the mean score of inflammation,

Table 1
Effects of EPA on body weight, liver weight, serum and hepatic laboratory parameters.

Parameters	2 weeks			8 weeks			14 weeks		
	SP	HFC	HFC + EPA	SP	HFC	HFC + EPA	SP	HFC	HFC + EPA
Body weight (g)	263 ± 19	242 ± 13[a]	221 ± 15[b]	314 ± 20	268 ± 14[a]	251 ± 18	336 ± 22	277 ± 19[a]	251 ± 26
Liver weight (g)	7.3 ± 0.7	11.6 ± 3.8[a]	10.6 ± 0.8	8.3 ± 0.8	34.6 ± 3.8[a]	32.3 ± 2.1	9.3 ± 0.7	37.5 ± 4.9[a]	47.9 ± 4.3[b]
Relative liver weight (%)	2.8 ± 0.1	4.8 ± 1.5[a]	4.8 ± 0.1	2.6 ± 0.1	12.9 ± 1.2[a]	12.9 ± 0.6	2.8 ± 0.1	13.5 ± 1.3[a]	19.1 ± 0.6[b]
Serum									
TG (mg/dl)	36 ± 13	41 ± 5	29 ± 6[b]	37 ± 9	29 ± 11	24 ± 7	42 ± 8	79 ± 63	115 ± 106
AST (IU/l)	122 ± 12	144 ± 11[a]	154 ± 20	105 ± 10	545 ± 209[a]	401 ± 300	118 ± 21	1121 ± 320[a]	856 ± 271
ALT (IU/l)	47 ± 4	94 ± 15[a]	111 ± 14	52 ± 4	220 ± 66[a]	254 ± 146	50 ± 6	387 ± 87[a]	300 ± 88
γ-GTP (IU/l)	1.5 ± 0[c]	1.5 ± 0[c]	1.5 ± 0[c]	1.5 ± 0[c]	10.3 ± 2[a]	4.8 ± 1[b]	1.5 ± 0[c]	13.8 ± 3[a]	12.9 ± 7
IL-6 (pg/ml)	44 ± 35	123 ± 31[a]	121 ± 100	29 ± 12	240 ± 65[a]	126 ± 60[b]	88 ± 69	203 ± 37[a]	140 ± 77
TNF-α (pg/ml)	1.3 ± 1.9	7.2 ± 3.3[a]	2.5 ± 0.7[b]	0.5 ± 0.5	13.0 ± 3.3[a]	11.1 ± 1.2	2.1 ± 2.2	15.8 ± 6.2[a]	21.1 ± 4.2
Adiponectin (μg/ml)	5.4 ± 0.4	7.1 ± 1.0[a]	6.7 ± 2.1	5.2 ± 1.0	5.1 ± 2.0	7.8 ± 1.0[b]	6.2 ± 0.8	4.0 ± 0.6[a]	5.7 ± 2.1
TNF-α/Adiponectin (×10^6)	0.2 ± 0.4	1.0 ± 0.5[a]	0.4 ± 0.2[b]	0.1 ± 0.1	2.8 ± 1.1[a]	1.4 ± 0.2[b]	0.4 ± 0.4	4.2 ± 1.9[a]	4.1 ± 1.3
Liver									
TG (mg/g liver)	19 ± 3	56 ± 27[a]	56 ± 14	18 ± 5	36 ± 12[a]	18 ± 7[b]	15 ± 3	28 ± 7[a]	24 ± 9

Body weight is also used elsewhere (Kitamori et al., in press). Values are expressed as mean ± standard deviation. [a]$P<0.05$ vs. SP-fed group, [b]$P<0.05$ vs. HFC-fed group. [c]Detection limit was 3.0 IU/l. When values were below the detection limit, we used 1.5 IU/l as the result of detection. Abbreviations: SP, stroke-prone; HFC, high fat-cholesterol; EPA, eicosapentaenoic acid; TG, triglyceride; AST, aspartate aminotransferase; ALT, alanine aminotransferase; γ-GTP, γ-glutamyl transpeptidase; IL-6, interleukin-6; TNF-α, tumor necrosis factor-α.

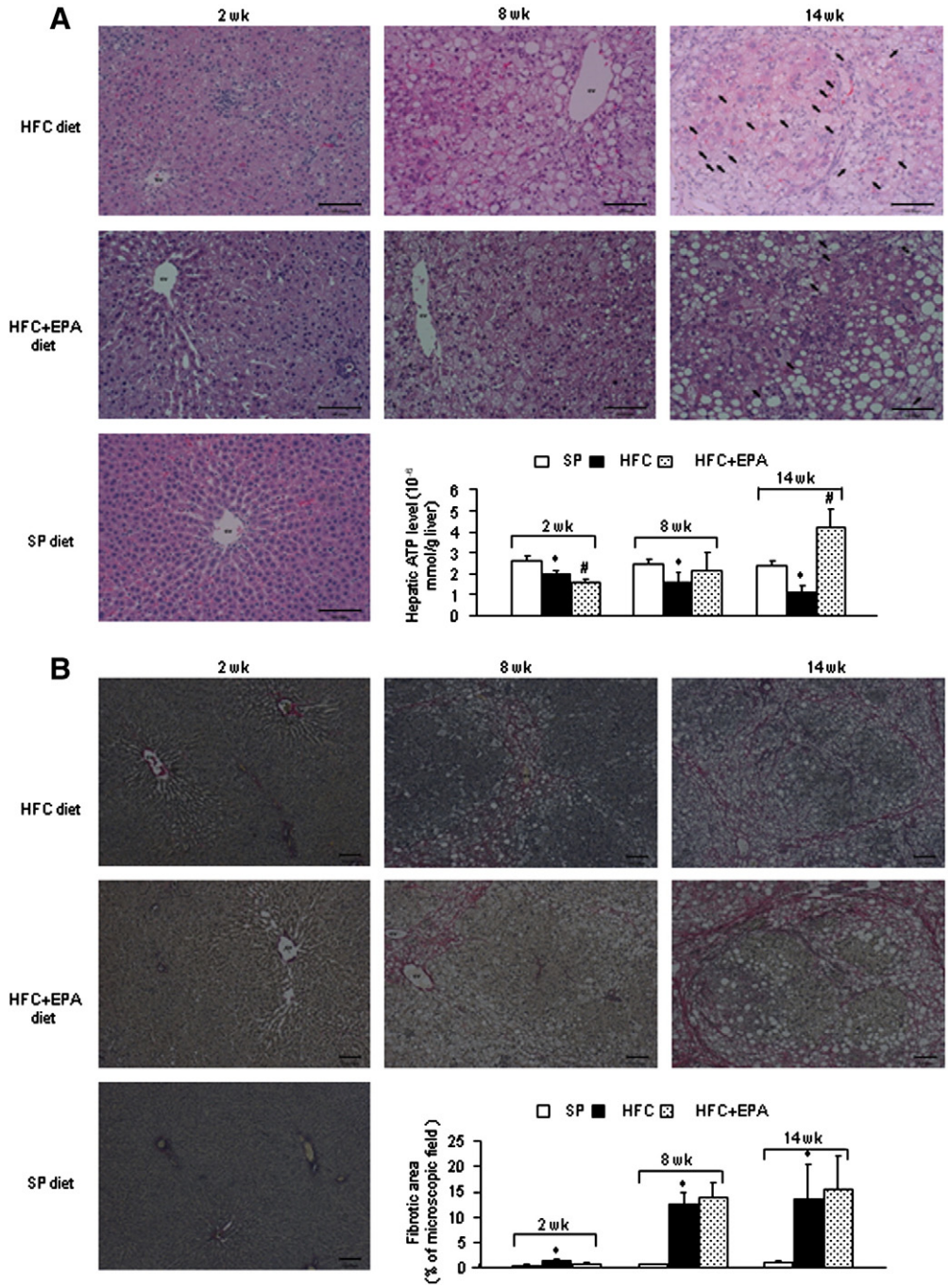

Fig. 1. The liver histology, hepatic ATP levels and fibrotic area evaluation of rats fed the SP or the HFC diet with or without EPA. (A) Representative images of hematoxylin and eosin staining (magnification: 200×; arrows indicate ballooning degeneration) and a bar graph of hepatic ATP levels. (B) Representative images of Elastic Van Gieson staining (magnification: 100×) and a bar graph of the quantification of fibrosis. CV, central vein. Scale bar: 100 μm. *$P<0.05$ vs. SP group, #$P<0.05$ vs. HFC group. Abbreviations: ATP, adenosine triphosphate; HFC, high fat-cholesterol; SP, stroke-prone; EPA, eicosapentaenoic acid.

from 1.2 ± 0.2 to 0.9 ± 0.1, which was partially attributed to improvements in the serum levels of inflammatory cytokines. At 8 weeks, the EPA-treated rats exhibited reduced macrovesicular steatosis supported by decreased hepatic TG deposition and at 14 weeks, they exhibited a decreased mean score of ballooning degeneration—a phenotype of cell death.

The EVG-staining showed that rats fed with the HFC diet, regardless of EPA, developed moderate fibrosis mainly in the perivenular to pericellular areas starting from 8 weeks and progressed to bridging fibrosis at 14 weeks (Fig. 1B). Evaluation of the fibrotic areas revealed that the HFC diet induced severe fibrosis compared to the control diet starting from 8 weeks onward. Unfortunately, no attenuation in fibrotic progression was detected after EPA supplementation.

The effects of EPA on hepatic ATP levels

Because the EPA decreased the numbers of ballooned hepatocytes and appeared to maintain more active cells at 14 weeks, we measured hepatic ATP levels (Fig. 1A). The rats fed with the HFC diet alone exhibited a persistently lower ATP levels than that of rats fed the

Table 2
Liver histological scores in rats treated with SP diet, HFC diet with or without EPA.

	2 weeks			8 weeks			14 weeks		
	SP	HFC	HFC + EPA	SP	HFC	HFC + EPA	SP	HFC	HFC + EPA
Steatosis	0.6 ± 0.3	3.0 ± 0.1[a]	3.0 ± 0.0	1.0 ± 0.6	3.0 ± 0.0[a]	3.0 ± 0.0	1.2 ± 0.5	3.0 ± 0.0[a]	3.0 ± 0.0
Lobular inflammation	0.8 ± 0.2	1.2 ± 0.2[a]	0.9 ± 0.1[b]	0.8 ± 0.2	1.0 ± 0.4	1.3 ± 0.2	1.1 ± 0.1	1.7 ± 0.3[a]	1.4 ± 0.4
Ballooning	0.0 ± 0.0	0.2 ± 0.1[a]	0.1 ± 0.2	0.0 ± 0.0	0.5 ± 0.2[a]	0.6 ± 0.1	0.0 ± 0.0	0.8 ± 0.2[a]	0.6 ± 0.1[b]
NAS	1.4 ± 0.4	4.3 ± 0.3[a]	4.0 ± 0.2[b]	1.8 ± 0.7	4.6 ± 0.4[a]	4.9 ± 0.3	2.3 ± 0.5	5.5 ± 0.4[a]	5.0 ± 0.4
Macrovesicular steatosis	0.0 ± 0.0	0.0 ± 0.0	0.0 ± 0.0	0.0 ± 0.0	0.9 ± 0.3[a]	0.2 ± 0.3[b]	0.0 ± 0.0	0.9 ± 0.3[a]	0.8 ± 0.2

Values are expressed as mean ± standard deviation. [a]$P<0.05$ vs. SP-fed group, [b]$P<0.05$ vs. HFC-fed group using Mann–Whitney *U* test. Abbreviations: SP, stroke-prone; HFC, high fat-cholesterol; EPA, eicosapentaenoic acid; NAS, NAFLD activity score.

control diet. Upon supplementation with EPA, the ATP levels exhibited a sharp increase at 14 weeks relative to the HFC diet alone or the control diet, although a decreased level was detected at 2 weeks.

The effects of EPA on fatty acid metabolism

Given the improvements in the hepatic TG accumulation and macrovesicular steatosis, the fatty acid metabolism pathways were investigated. The nuclear mature sterol regulatory element-binding protein 1c (SREBP-1c) activates the transcription of lipogenic genes (Ferre and Foufelle, 2010). The administration of EPA significantly inhibited the HFC-induced increase in the SREBP-1 mRNA at the treatment endpoint (Fig. 2A) but did not significantly influence the nuclear levels of SREBP-1c protein (Fig. 2B). We also evaluated specific SREBP-1c target genes and found that the HFC diet-fed rats exhibited progressively elevated mRNA levels of fatty acid synthase (FAS) and stearoyl-CoA desaturase 1 (SCD1) compared to the control diet-fed rats during the whole treatment period. The EPA treatment significantly decreased the levels of FAS mRNA at 2 and 14 weeks and of SCD1 mRNA at 14 weeks compared to the HFC diet alone (Fig. 2A). Protein analysis revealed that the HFC diet resulted in higher FAS protein levels at 2 and 8 weeks compared to the control diet. However, treatment with EPA did not significantly affect the protein levels of these lipogenic enzymes (Fig. 2B). The effects on the acetyl-CoA carboxylase-α (ACCα) protein were similar to those of the FAS protein (not shown). The diacylglycerol acyltransferase-2 (DGAT2) protein, a more potent DGAT that catalyzes the final step in TG synthesis, was not suppressed by the administration of EPA, although the EPA inhibited its mRNA level relative to HFC diet alone at 8 and 14 weeks (Fig. 2A and B). The alterations in DGAT1 protein levels were similar to those of DGAT2 protein levels (not shown). These results suggest that the administration of EPA may not down-regulate the lipogenic pathways examined in our study.

The peroxisome proliferator-activated receptor α (PPARα) plays a pivotal role in the pathogenesis of steatosis due to its ability to orchestrate fatty acid oxidation (Ishii et al., 2009). The HFC diet suppressed PPARα mRNA throughout the treatment period compared to the control diet. The administration of EPA further reduced the mRNA levels at 14 weeks (Fig. 3A). Conversely, the feeding of the HFC diet itself, regardless of the administration of EPA, significantly elevated the protein expression at 2 weeks, but did not influence it thereafter (Fig. 3B). The measurements of the representative enzymes for fatty acid oxidation revealed that the HFC diet-fed rats expressed lower levels of carnitine palmitoyltransferase 1 (CPT1), very long chain acyl-CoA dehydrogenase (VLCAD) and peroxisomal bifunctional protein (PH) than did the control diet-fed rats at 8 and 14 weeks (Fig. 3B). Importantly, the EPA treatment inhibited the HFC diet-induced decrease in all three proteins at 8 weeks, supporting the notion that the administration of EPA reduced hepatic TG accumulation and macrovesicular steatosis by accelerating fatty acid oxidation in this model.

The effects of EPA on inflammation

NF-κB is a major regulator of the inflammatory process (Elsharkawy and Mann, 2007). Investigation of the pathways that activate NF-κB (Fig. 4) showed that the HFC diet markedly increased protein levels of the inhibitor of κB (IκB) kinase α/β (IKKα/β) at 8 and 14 weeks, phosphorylated IKKβ (phospho-IKKβ) at 8 weeks, IκBα at each term, and, particularly, phosphorylated IκBα (phospho-IκB-α) at 2 weeks compared to the control diet. This activation eventually resulted in the nuclear accumulation of p50 protein from 2 weeks onward and p65 at 2 weeks in HFC diet-fed rats. The administration of EPA significantly inhibited the HFC diet-induced increase in IKKα/phospho-IKKα at 8 weeks. Although EPA did not affect the IKKβ/phospho-IKKβ relative to the HFC diet alone, EPA treatment suppressed IκBα/phospho-IκB-α at 2 and 8 weeks compared to the HFC diet alone. We detected a decrease in the nuclear accumulation of p50 and p65 at 2 weeks, consistent with the histopathological inhibition of inflammation at that time. Interestingly, p65 DNA binding activity (Fig. 4) did not improve in the HFC diet-fed rats after EPA intake at 2 weeks, but rather exhibited elevation at 8 and 14 weeks. The HFC diet alone also induced monocyte chemoattractant protein-1 (MCP-1), which is an NF-κB downstream target (Fig. 4). The administration of EPA, however, did not further alter MCP-1.

The mitogen-activated protein kinase (MAPK) signal transduction pathways play a crucial role in many aspects of the inflammatory response (Hommes et al., 2003). Three well-characterized classes of MAPKs, which include the extracellular signal-regulated kinases (ERKs), c-Jun amino-terminal kinases (JNKs) and p38 MAPK, were further assessed by western blot (Fig. 5). The ERK1 protein levels were higher in the HFC diet-fed rats than in the control rats at 8 and 14 weeks, whereas the activated form of ERK1 was extremely low regardless of diet and EPA administration, except in a few cases in the HFC-diet group at 14 weeks and in the EPA-treated group at 8 weeks. As a result, the EPA-treated group exhibited increased phospho-ERK1 levels at 8 weeks. Differences in the levels of ERK2/phospho-ERK2 were not detected between the groups. Conversely, EPA treatment inhibited the HFC-induced increase of JNK p46 levels at 14 weeks, although no changes in phospho-JNK p46 or in JNK p54/phospho-JNK p54 were detected. Additionally, the levels of p38/phospho-p38 were comparable between the groups (data not shown). These findings indicate that the MAPK pathways might not be major contributors to liver inflammation and steatohepatitis in our study.

Discussion

In this study, histopathological evaluation revealed that the co-administration of EPA with an HFC diet partially ameliorated diet-induced inflammation and macrovesicular steatosis at 2 and 8 weeks, respectively, which is consistent with previous reports (Kajikawa et al., 2009a, 2009b, 2010; Tanaka et al., 2010). The administration of EPA also improved the degree of ballooning degeneration detected

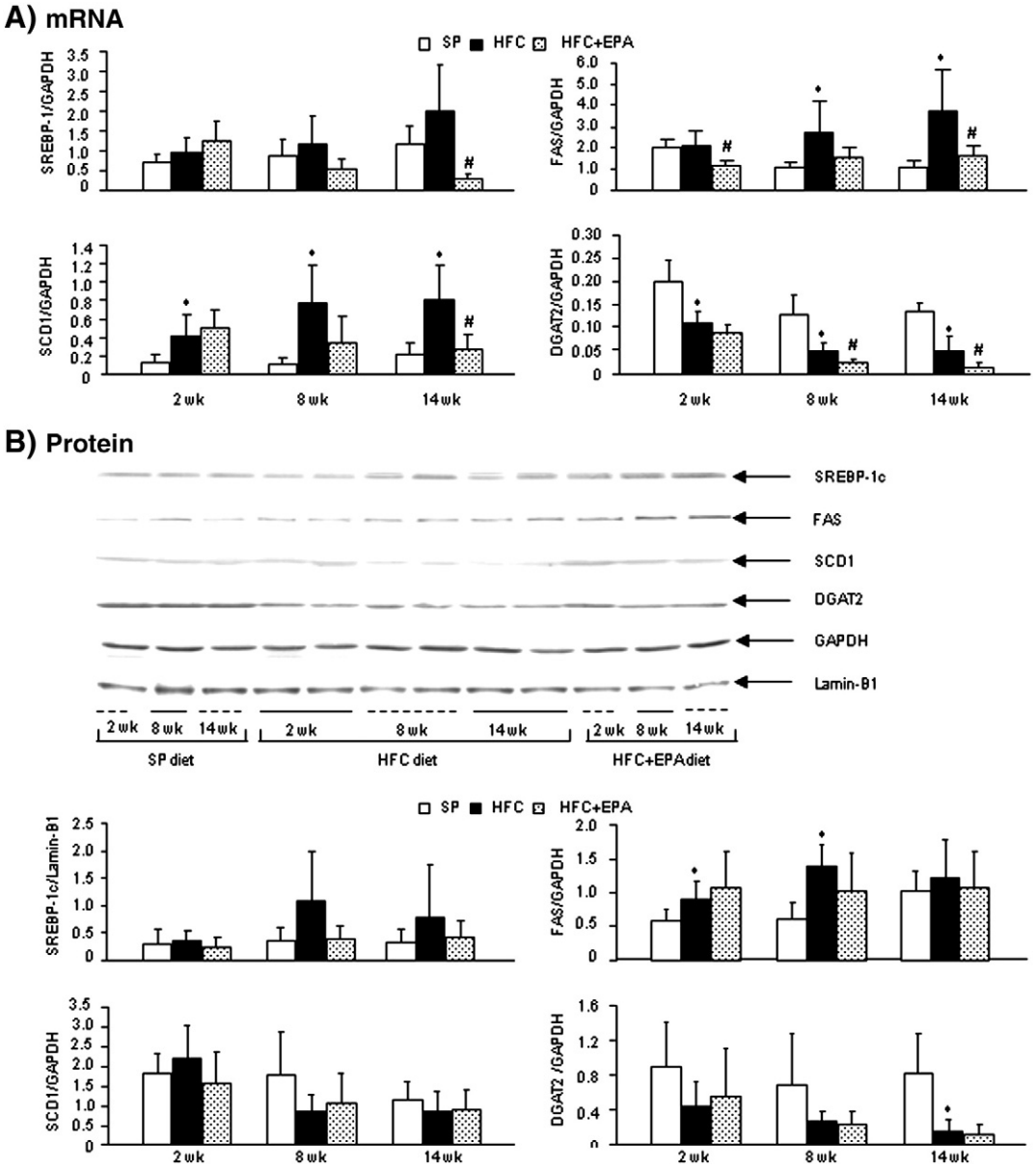

Fig. 2. The effects of EPA on the de novo lipogenesis and triglyceride biosynthesis. (A) Real-time quantitative PCR of SREBP-1, FAS, SCD1 and DGAT2. The EPA-treated rats exhibited decreased SREBP-1 and SCD1 expressions at 14 weeks, inhibited FAS mRNA at 2 and 14 weeks, and reduced DGAT2 mRNA at 8 and 14 weeks, relative to rats fed the HFC-only diet. (B) The hepatic SREBP-1c, FAS, SCD1 and DGAT2 protein levels were analyzed by western blot. GAPDH or Lamin-B1 was used as loading control. The administration of EPA alongside the HFC diet did not significantly alter protein levels of these enzymes (n = 6/group, $^{*}P<0.05$ vs. SP group; $\#P<0.05$ vs. HFC group). Abbreviations: SREBP-1c, sterol regulatory element-binding protein 1c; FAS, fatty acid synthase; SCD1, stearoyl-CoA desaturase 1; DGAT2, diacylglycerol acyltransferase-2; GAPDH, glyceraldehyde-3-phosphate dehydrogenase.

at 14 weeks, which to our knowledge, is a novel finding. Although at 14 weeks the HFC diet induced comparable chicken-wire fibrosis, regardless of EPA, there were fewer ballooned hepatocytes in the rats that were administered the EPA supplement, which corresponded to a significant EPA-induced elevation in hepatic ATP levels at 14 weeks. Thus, the administration of EPA played a significant role in the pathogenesis of fibrotic steatohepatitis. All of these features encouraged us to unravel the potential mechanisms of the roles of EPA in fibrotic steatohepatitis.

The EPA-induced inhibition of ballooning degeneration suggests that EPA might play a role in maintaining cell survival. Normal differentiated cells rely primarily on mitochondrial oxidative phosphorylation to produce ATP to maintain their viability and normal cellular functions (Pike et al., 2011). ATP depletion may be an important cause of hepatocellular injury in the steatotic liver (Neuschwander-Tetri and Caldwell, 2003). Indeed, hepatic ATP depletion during NASH development has also been previously demonstrated in a rodent model (Serviddio et al., 2008). Likewise, our fibrotic steatohepatitis model exhibited lower hepatic ATP levels than the controls, suggesting the presence of mitochondrial dysfunction and impaired energy homeostasis. A recent study of steatotic HepG2 cells cultured with fatty acids revealed that incubation of the cells with EPA improved their abnormal mitochondrial morphology and increased the levels of ATP (Zhang et al., 2011). In this study, the administration of EPA sharply elevated hepatic ATP content at 14 weeks concurrently with a pathological inhibition of hepatocyte ballooning. These functions have not been reported yet in the liver under severe fibrotic progression and suggest that EPA treatment might reduce HFC diet-induced mitochondrial dysfunction and restore hepatic ATP stores, thereby protecting hepatocytes from necrosis. These effects might account for the increased liver weight observed at 14 weeks in the EPA group, whereas the liver weights did not increase in the HFC-diet only group at 14 weeks compared to those at 8 weeks.

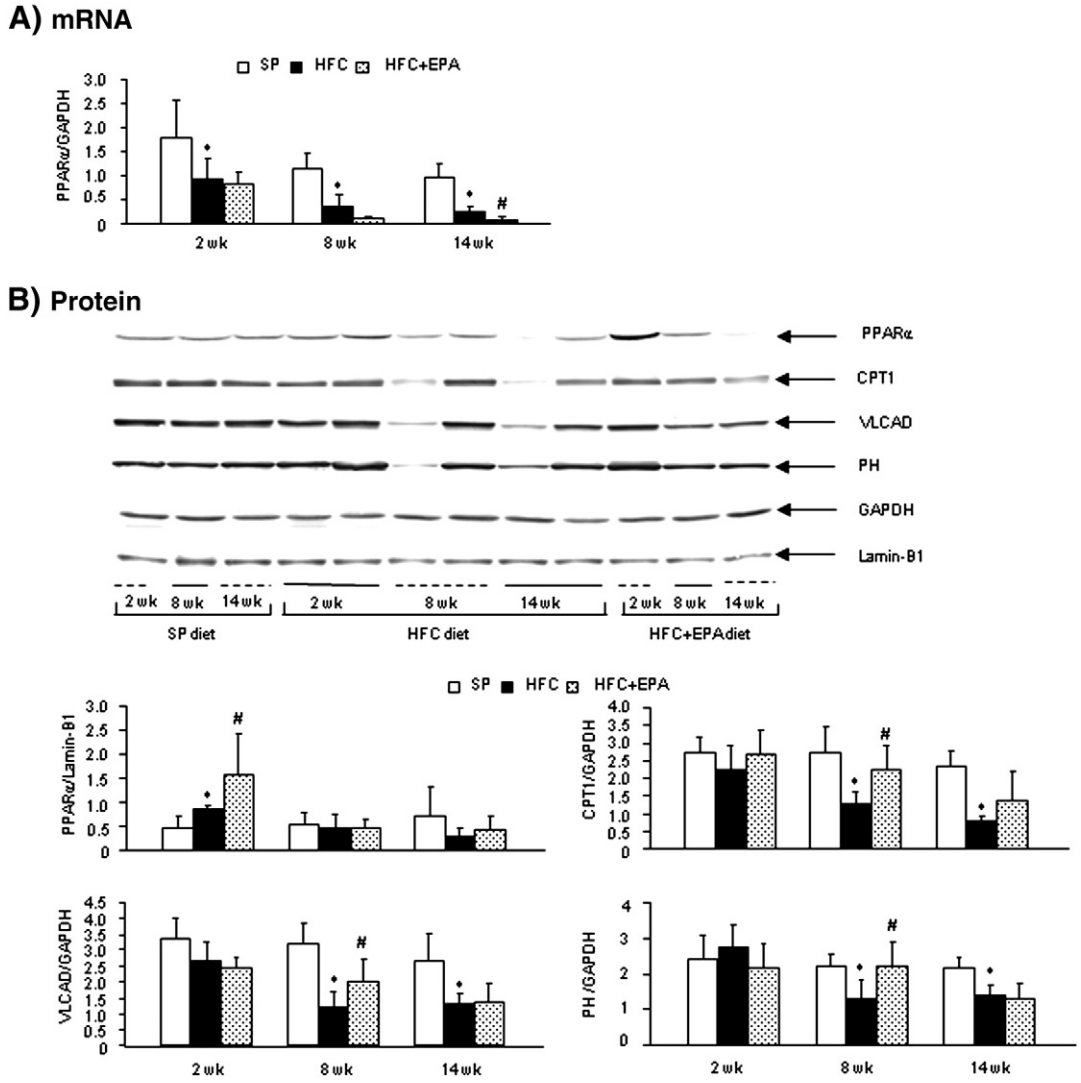

Fig. 3. The effects of EPA on fatty acid β-oxidation. (A) The hepatic mRNA levels of PPARα. The rats fed with the HFC diet, regardless of EPA, exhibited persistently decreased PPARα mRNA, relative to control diet-fed rats. (B) Western blot analysis of PPARα, CPT1, VLCAD and PH. GAPDH or Lamin-B1 was used as loading control. The rats that were fed the HFC diet with or without EPA had higher PPARα protein levels only at 2 weeks compared to control diet-fed rats. The EPA treatment significantly inhibited HFC-induced reduction in CPT1, VLCAD and PH at 8 weeks (n = 6/group, $^{*}P<0.05$ vs. SP group; $\#P<0.05$ vs. HFC group). Abbreviations: PPARα, peroxisome proliferator-activated receptor α; CPT1, carnitine palmitoyltransferase 1; VLCAD, very long chain acyl-CoA dehydrogenase; PH, peroxisomal bifunctional protein.

Steatosis is the excessive accumulation of triglycerides in the liver. The imbalance of lipid availability and lipid disposal is a critical determinant in the pathogenesis of steatosis (Ferre and Foufelle, 2010). We investigated two aspects of the underlying mechanisms responsible for the steatosis-attenuating effect of EPA: de novo lipogenesis and fatty acid oxidation. EPA treatment stimulated β-oxidation in both mitochondria and peroxisomes at 8 weeks by inhibiting the HFC-induced decrease in protein expression of enzymes including CPT1, VLCAD and PH. Several studies have demonstrated that EPA treatment can increase mitochondrial and peroxisomal fatty acid oxidations. In particular, a recent NASH model using Medaka revealed that the administration of EPA mitigated high fat diet-induced disease by restoring normal mitochondrial β-oxidation (Matsumoto et al., 2010), which is confirmed by our findings. Therefore, we conclude that the EPA-mediated reduction of hepatic TG accumulation and attenuation of macrovesicular steatosis at 8 weeks may be attributed to the enhanced mitochondrial and peroxisomal β-oxidations. Additionally, although a previous study has suggested that EPA is an active ligand for PPARα, a major transcription factor that regulates fatty acid β-oxidation (Ishii et al., 2009; Pawar and Jump, 2003), the administration of EPA did not significantly induce PPARα protein in the model employed in this study, similar to previous observations of mice with steatosis (Tanaka et al., 2010). Alternatively, SREBP-1c is a transcription factor that regulates lipogenic enzymes such as ACCα, FAS and SCD1 (Ferre and Foufelle, 2010). However, according to the proposed pathways for major lipid metabolism (Zhou et al., 2008), the decreased levels of SCD1 and DGAT2 in the HFC diet-fed group might be indicative of mitochondrial dysfunction. Several animal experiments have demonstrated that the administration of EPA improved hepatic steatosis by inhibiting mRNA (Ishii et al., 2009; Kajikawa et al., 2009a,b; Matsumoto et al., 2010) or protein (Tanaka et al., 2010) levels of SREBP-1c and lipogenic enzymes. Although we observed a marked down-regulation of these enzymes at the mRNA level, we failed to observe a significant role for EPA at the protein level. The administration of EPA also did not influence TG synthesis via regulation of DGAT2. Thus, we conclude that the EPA-induced reduction of hepatic TG accumulation and attenuation of histological macrovesicular steatosis in our study was not attributed to inhibition of lipogenesis.

EPA has been identified as an anti-inflammatory PUFA (Kim et al., 2008; Zhao et al., 2004). In this study, the inhibition of inflammation by EPA was histologically detected as early as 2 weeks, with

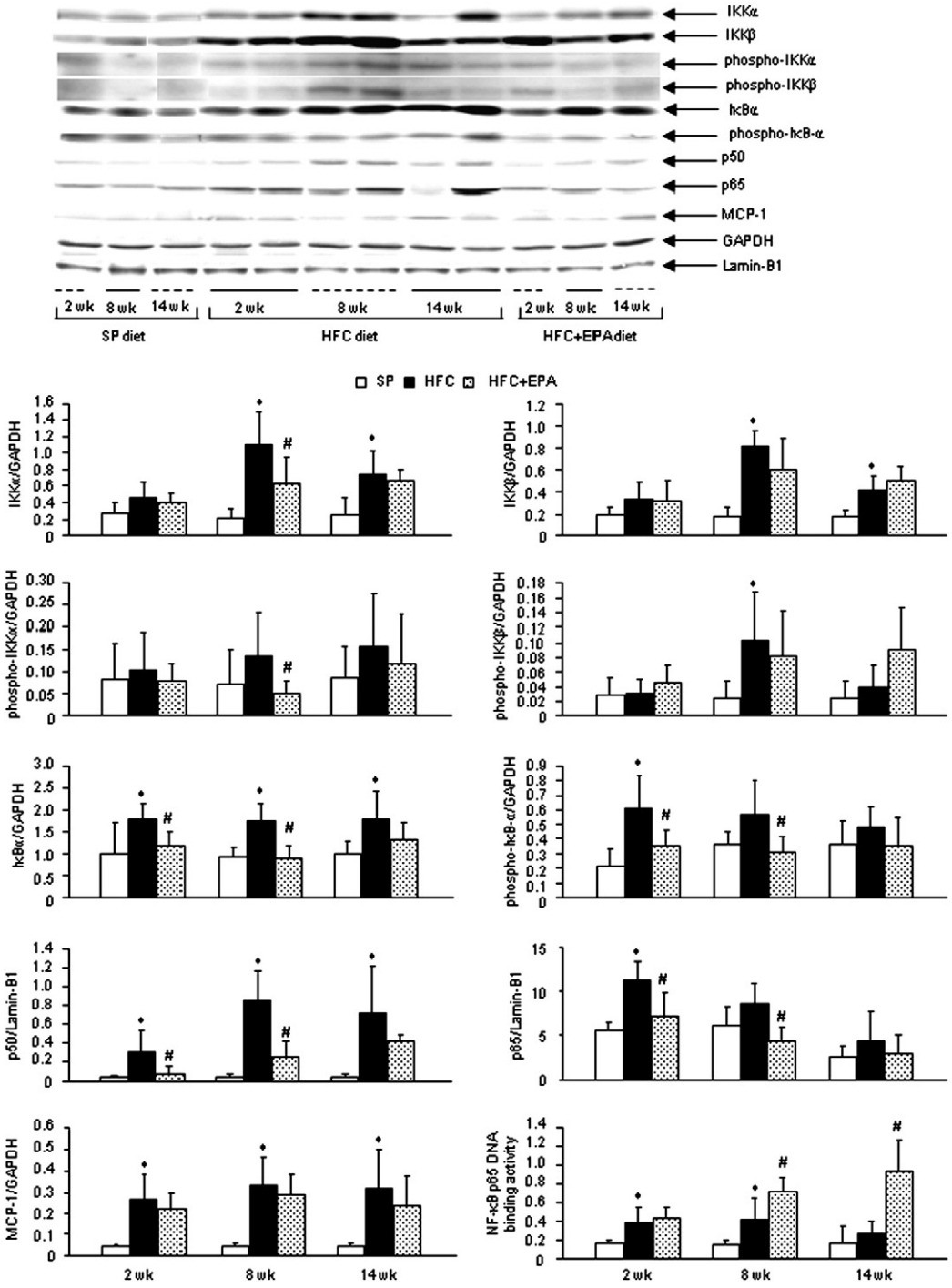

Fig. 4. The effects of EPA on the activation of the NF-κB pathway. Protein expressions of IKKα/β, IκBα and their phosphorylated forms, NF-κB p50 and p65 subunits, and targeted MCP-1 are displayed. GAPDH or Lamin-B1 used as loading control. The EPA treatment inhibited the HFC-induced increase in IκBα/phospho-IκB-α, resulting in decreased p50 and p65 at 2 and 8 weeks. It also inhibited IKKα/phospho-IKKα at 8 weeks, but did not influence MCP-1 levels. The p65 DNA binding activity is also shown. Interestingly, the EPA did not affect the p65 activity at 2 weeks (n = 6/group, $^{*}P<0.05$ vs. SP group; #$P<0.05$ vs. HFC group). Abbreviations: IKKα/β, inhibitor of κB kinase α/β; phospho-IKKα/β, phosphorylated IKKα/β; IκBα, inhibitor of κB-α; phospho-IκB-α, phosphorylated IκBα; NF-κB, nuclear factor-κB; MCP-1, monocyte chemoattractant protein-1.

a concomitant decrease in TNF-α and increase in adiponectin levels in the serum relative to HFC diet-only groups in early stages, consistent with previous reports (Ishii et al., 2009; Kajikawa et al., 2009b, 2010). At 8 weeks, the administration of EPA also suppressed the serum levels of inflammatory cytokine, IL-6. The NF-κB signaling pathway plays a role in the pathogenesis of a wide variety of conditions affecting the liver, such as steatohepatitis (Robinson and Mann, 2010). NF-κB, commonly referred to as its p65:p50 protein heterodimer, accumulates in the initiation phase of inflammation. The IKKβ-mediated phosphorylation of IκBα liberates NF-κB, promoting its transport into the nucleus, which constitutes a pivotal event in activation of the classic NF-κB pathway (Elsharkawy and Mann, 2007; Robinson and Mann, 2010). Here, the HFC diet increased IKKα/β levels and stimulated the phosphorylated states of IKKβ and IκBα, thereby elevating the nuclear levels of p65 and p50 proteins. Furthermore, p65 DNA binding activity was increased in early stages relative to controls. The inflammatory score declined from 2 to 8 weeks in HFC diet-fed rats. However, between 8 and 14 weeks, the score increased in only the HFC diet-fed

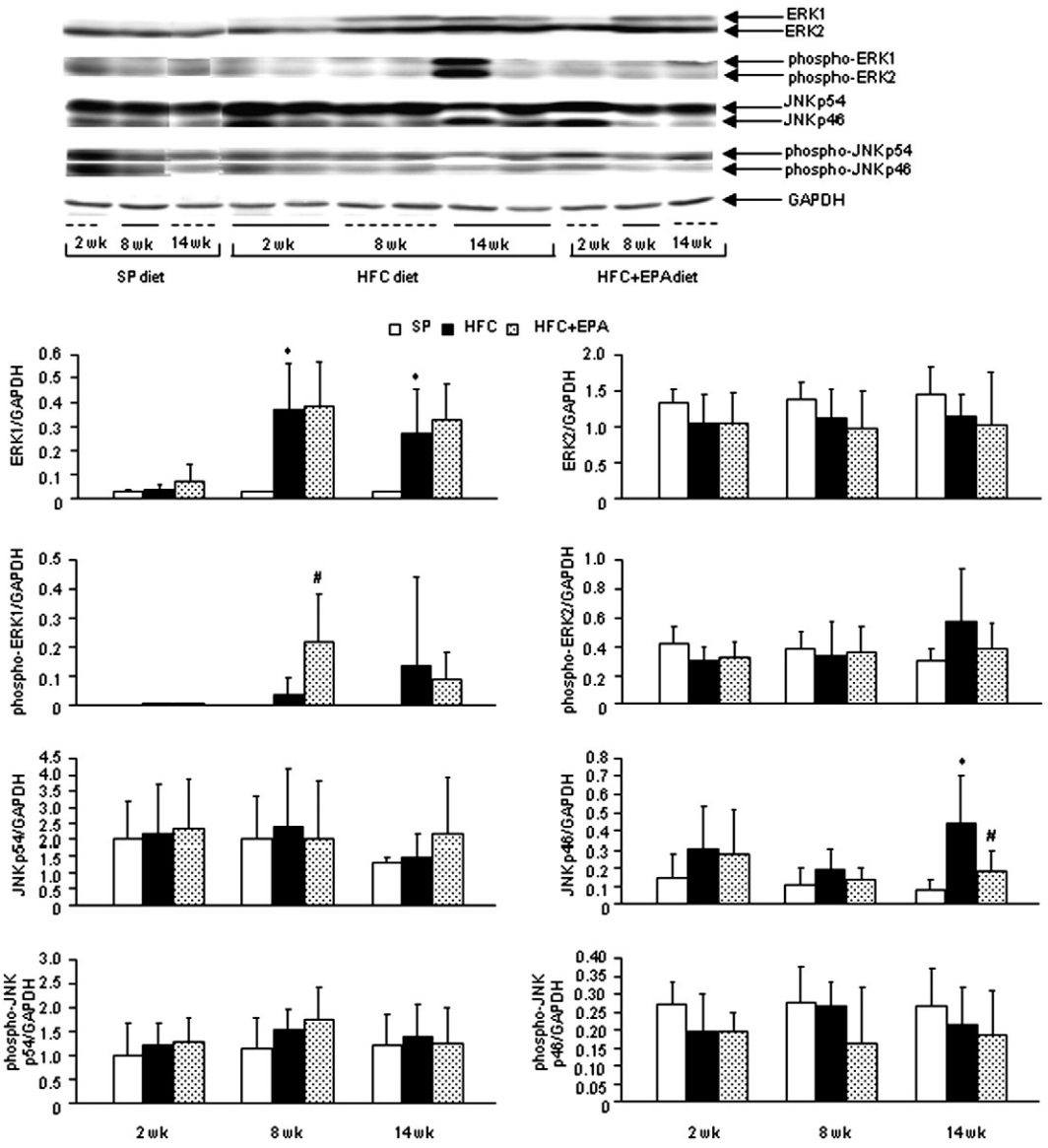

Fig. 5. The effects of EPA on the MAPK signaling pathways. The protein levels of ERK1/2, JNK p54/p46, and their corresponding phosphorylated forms are shown. GAPDH was used as loading control. EPA treatment increased phospho-ERK1 at 8 weeks, compared to the HFC diet-alone group. EPA inhibited the HFC-induced increase of JNK p46 at 14 weeks (n = 6/group, *P<0.05 vs. SP group; #P<0.05 vs. HFC group). Abbreviations: MAPK, mitogen-activated protein kinase; ERK1/2, extracellular signal-regulated kinase 1/2; phospho-ERK1/2, phosphorylated ERK1/2; JNK, c-Jun amino-terminal kinases; phospho-JNK, phosphorylated JNK.

group, possibly due to necrosis, which results in the rupture of hepatocytes and consequential release of the cellular components that stimulate the acute inflammation response (Sokol, 2002). EPA reportedly inhibits NF-κB activation in various cells (Kim et al., 2008; Zhao et al., 2004). As an anti-inflammatory PUFA, EPA may predominantly affect the abundant pro-inflammatory components of the p65:p50 heterodimers of the NF-κB family, accounting for the suppression of the nuclear p65 and p50 subunits at 2 and 8 weeks. This inhibition was a phospho-IκB-α-dependent event (Zhao et al., 2004), leading to improved inflammation in histopathology at 2 weeks. Unexpectedly, EPA did not affect the DNA binding activity of p65 at 2 weeks. The delayed action of EPA on p65 binding activity might occur between 2 and 8 weeks, as the duration of NF-κB activation was prolonged after exposure to EPA (Ross et al., 2003). The increased activity observed at 8 and 14 weeks of EPA treatment could not exclude the possibility of a partial role of NF-κB in liver regeneration following liver injury, as was indicated by elevated ATP levels and inhibited ballooning (FitzGerald et al., 1995). Because the IκBα gene is up-regulated by the activation of NF-κB (Chiao et al., 1994; Scott et al., 1993), the induction of IκBα was preceded by activation of NF-κB in the HFC diet-fed group. The decrease in NF-κB activation by EPA may slow the repletion of IκBα, contrary to what was observed in the HFC-diet group. Taken together, the EPA treatment for 2 weeks histologically ameliorated inflammation mainly by preventing the HFC diet-induced increase in serum TNF-α, TNF-α/adiponectin and NF-κB pathway activation.

Additionally, MCP-1 was reportedly up-regulated in livers of NASH patients, functioning as a chemotactic factor for the recruitment of monocytes during inflammation (Bertola et al., 2010). We found that MCP-1 was greatly induced in HFC diet-fed rats with steatohepatitis. Although EPA did not influence the levels of MCP-1, it changed the composition of NF-κB. Given a previous study (Diaz Encarnacion et al., 2011), we propose that the inhibition of MCP-1 production by EPA treatment not only involves the suppression of NF-κB but also other alternative intracellular signaling pathways.

Finally, MAPKs such as JNK and p38 are regarded as central mediators in obesity and insulin resistance (Gao et al., 2010; Hirosumi et al., 2002). The activation of MAPKs has been reported to promote the development of steatohepatitis with hepatic insulin resistance

(Schattenberg et al., 2006) and to be critically involved in a high fat dietary model of obesity-associated NAFLD (Sinha-Hikim et al., 2011). Conversely, we did not observe the activation of ERK1/2, JNK or p38 by the HFC diet or their inhibition by EPA in our study. These findings suggest that the MAPK pathways might not be responsible for the initiation of the inflammatory response in steatohepatitis in our current model.

Unexpectedly, no EPA-mediated attenuation of fibrosis was histologically detected. A previous report has shown that the inhibition of DGAT2 in a NASH animal model improved steatosis but exacerbated hepatic damage and fibrosis, suggesting that hepatic TG accumulation may be a protective mechanism that prevents progressive fibrosis (Yamaguchi et al., 2007). EPA inhibited HFC diet-induced hepatic TG accumulation at 8 weeks, suggesting that the decreased TG in the EPA group may further exacerbate fibrosis. Our model itself, which is unique in its development of predominant bridging fibrosis, might be another pivotal factor that constrained the efficacy of EPA treatment. Nonetheless, EPA appeared to inhibit cell death, which is a causal factor in fibrogenesis, accompanied by restoration of hepatic ATP levels and ballooning inhibition.

Conclusions

In conclusion, the administration of EPA can ameliorate the initial inflammation and steatosis in SHRSP5/Dmcr rats fed with an HFC diet. In the phase of progressive fibrosis, EPA replenishes the hepatic ATP levels and reduces hepatocellular ballooning, and through a new-found ability, restores mitochondrial energy homeostasis to inhibit cell death. Taken together, our results provide evidence that EPA may constitute a therapeutic agent for early-stage steatohepatitis by improving inflammation and steatosis. Lastly, our study provides new insights into the roles of EPA in hepatic ATP depletion in the fibrotic liver.

Supplementary data to this article can be found online at http://dx.doi.org/10.1016/j.lfs.2012.04.029.

Conflict of interest statement

The authors declare that there are no conflicts of interest.

Acknowledgments

We are grateful to the Mochida Pharmacy (Tokyo, Japan) for generously providing the EPA agent. This study was supported in part by a Grant-in-Aid for Scientific Research (B23390161) from the Japan Society for the Promotion of Science.

References

Bertola A, Bonnafous S, Anty R, Patouraux S, Saint-Paul MC, Iannelli A, et al. Hepatic expression patterns of inflammatory and immune response genes associated with obesity and NASH in morbidly obese patients. PLoS One 2010;5:e13577.
Chiao PJ, Miyamoto S, Verma IM. Autoregulation of I kappa B alpha activity. Proc Natl Acad Sci U S A 1994;91:28–32.
Cortez-Pinto H, Machado M. Impact of body weight, diet and lifestyle on nonalcoholic fatty liver disease. Expert Rev Gastroenterol Hepatol 2008;2:217–31.
de Alwis NM, Day CP. Non-alcoholic fatty liver disease: the mist gradually clears. J Hepatol 2008;48:S104–12.
Diaz Encarnacion MM, Warner GM, Cheng J, Gray CE, Nath KA, Grande JP. N-3 fatty acids block TNF-α-stimulated MCP-1 expression in rat mesangial cells. Am J Physiol Renal Physiol 2011;300:F1142–51.
Elsharkawy AM, Mann DA. Nuclear factor-κB and the hepatic inflammation-fibrosis-cancer axis. Hepatology 2007;46:590–7.
Enjoji M, Nakamuta M. Is the control of dietary cholesterol intake sufficiently effective to ameliorate nonalcoholic fatty liver disease? World J Gastroenterol 2010;16:800–3.
Ferre P, Foufelle F. Hepatic steatosis: a role for de novo lipogenesis and the transcription factor SREBP-1c. Diabetes Obes Metab 2010;12:83–92.
FitzGerald MJ, Webber EM, Donovan JR, Fausto N. Rapid DNA binding by nuclear factor κB in hepatocytes at the start of liver regeneration. Cell Growth Differ 1995;6:417–27.
Folch J, Lees M, Sloane Stanley GH. A simple method for the isolation and purification of total lipids from animal tissues. J Biol Chem 1957;226:497–509.
Gao D, Nong S, Huang X, Lu Y, Zhao H, Lin Y, et al. The effects of palmitate on hepatic insulin resistance are mediated by NAPDH oxidase 3-derived reactive oxygen species through JNK and p38MAPK pathways. J Biol Chem 2010;285:29965–73.
Hirosumi J, Tuncman G, Chang L, Gorgun CZ, Uysal KT, Maeda K, et al. A central role for JNK in obesity and insulin resistance. Nature 2002;420:333–6.
Hommes DW, Peppelenbosch MP, van Deventer SJ. Mitogen activated protein (MAP) kinase signal transduction pathways and novel anti-inflammatory targets. Gut 2003;52:144–51.
Ishii H, Horie Y, Ohshima S, Anezaki Y, Kinoshita N, Dohmen T, et al. Eicosapentaenoic acid ameliorates steatohepatitis and hepatocellular carcinoma in hepatocyte-specific Pten-deficient mice. J Hepatol 2009;50:562–71.
Kajikawa S, Harada T, Kawashima A, Imada K, Mizuguchi K. Highly purified eicosapentaenoic acid prevents the progression of hepatic steatosis by repressing monounsaturated fatty acid synthesis in high-fat/high-sucrose diet-fed mice. Prostaglandins Leukot Essent Fatty Acids 2009a;80:229–38.
Kajikawa S, Harada T, Kawashima A, Imada K, Mizuguchi K. Suppression of hepatic fat accumulation by highly purified eicosapentaenoic acid prevents the progression of D-galactosamine-induced hepatitis in mice fed with a high-fat/high-sucrose diet. Biochim Biophys Acta 2009b;1791:281–8.
Kajikawa S, Harada T, Kawashima A, Imada K, Mizuguchi K. Highly purified eicosapentaenoic acid ethyl ester prevents development of steatosis and hepatic fibrosis in rats. Dig Dis Sci 2010;55:631–41.
Kajikawa S, Imada K, Takeuchi T, Shimizu Y, Kawashima A, Harada T, et al. Eicosapentaenoic acid attenuates progression of hepatic fibrosis with inhibition of reactive oxygen species production in rats fed methionine- and choline-deficient diet. Dig Dis Sci 2011;56:1065–74.
Kim HH, Lee Y, Eun HC, Chung JH. Eicosapentaenoic acid inhibits TNF-α-induced matrix metalloproteinase-9 expression in human keratinocytes, HaCaT cells. Biochem Biophys Res Commun 2008;368:343–9.
Kitamori K, Naito H, Tamada H, Kobayashi M, Miyazawa D, Yasui Y, et al. Development of novel rat model for high-fat and high-cholesterol diet-induced steatohepatitis and severe fibrosis progression in SHRSP5/Dmcr. Environ Health Prev Med 2011. http://dx.doi.org/10.1007/s12199-011-0235-9.
Kleiner DE, Brunt EM, Van Natta M, Behling C, Contos MJ, Cummings OW, et al. Design and validation of a histological scoring system for nonalcoholic fatty liver disease. Hepatology 2005;41:1313–21.
Matsumoto T, Terai S, Oishi T, Kuwashiro S, Fujisawa K, Yamamoto N, et al. Medaka as a model for human nonalcoholic steatohepatitis. Dis Model Mech 2010;3:431–40.
Neuschwander-Tetri BA, Caldwell SH. Nonalcoholic steatohepatitis: summary of an AASLD single topic conference. Hepatology 2003;37:1202–19.
Pawar A, Jump DB. Unsaturated fatty acid regulation of peroxisome proliferator-activated receptor alpha activity in rat primary hepatocytes. J Biol Chem 2003;278:35931–9.
Pike LS, Smift AL, Croteau NJ, Ferrick DA, Wu M. Inhibition of fatty acid oxidation by etomoxir impairs NAPDH production and increases reactive oxygen species resulting in ATP depletion and cell death in human glioblastoma cells. Biochim Biophys Acta 2011;1807:726–34.
Ramdhan DH, Kamijima M, Wang D, Ito Y, Naito H, Yanagiba Y, et al. Differential response to trichloroethylene-induced hepatosteatosis in wild-type and PPARα-humanized mice. Environ Health Perspect 2010;118:1557–63.
Robinson SM, Mann DA. Role of nuclear factor κB in liver health and disease. Clin Sci (Lond) 2010;118:691–705.
Ross JA, Maingay JP, Fearon KC, Sangster K, Powell JJ. Eicosapentaenoic acid perturbs signalling via the NF kappaB transcriptional pathway in pancreatic tumour cells. Int J Oncol 2003;23:1733–8.
Schattenberg JM, Singh R, Wang Y, Lefkowitch JH, Rigoli RM, Scherer PE, et al. JNK1 but not JNK2 promotes the development of steatohepatitis in mice. Hepatology 2006;43:163–72.
Scott ML, Fujita T, Liou HC, Nolan GP, Baltimore D. The p65 subunit of NF-kappa B regulates I kappa B by two distinct mechanisms. Genes Dev 1993;7:1266–76.
Serviddio G, Bellanti F, Tamborra R, Rollo T, Romano AD, Giudetti AM, et al. Alterations of hepatic ATP homeostasis and respiratory chain during development of non-alcoholic steatohepatitis in a rodent model. Eur J Clin Invest 2008;38:245–52.
Sinha-Hikim I, Sinha-Hikim AP, Shen R, Kim H, Frence SW, Vaziri ND, et al. A novel cystine based antioxidant attenuates oxidative stress and hepatic steatosis in diet-induced obese mice. Exp Mol Pathol 2011;91:419–28.
Sokol RJ. Liver cell injury and fibrosis. J Pediatr Gastroenterol Nutr 2002;35:S7-S10.
Tanaka N, Sano K, Horiuchi A, Tanaka E, Kiyosawa K, Aoyama T. Highly purified eicosapentaenoic acid treatment improves nonalcoholic steatohepatitis. J Clin Gastroenterol 2008;42:413–8.
Tanaka N, Zhang X, Sugiyama E, Kono H, Horiuchi A, Nakajima T, et al. Eicosapentaenoic acid improves hepatic steatosis independent of PPARα activation through inhibition of SREBP-1 maturation in mice. Biochem Pharmacol 2010;80:1601–12.
Yamaguchi K, Yang L, McCall S, Huang J, Yu XX, Pandey SK, et al. Inhibiting triglyceride synthesis improves hepatic steatosis but exacerbates liver damage and fibrosis in obese mice with nonalcoholic steatohepatitis. Hepatology 2007;45:1366–74.
Yokoyama M, Origasa H, Matsuzaki M, Matsuzawa Y, Saito Y, Ishikawa Y, et al. Effects of eicosapentaenoic acid on major coronary events in hypercholesterolaemic patients (JELIS): a randomized open-label, blinded endpoint analysis. Lancet 2007;369:1090–8.
Zhang Y, Jiang L, Hu W, Zheng Q, Xiang W. Mitochondrial dysfunction during in vitro hepatocyte steatosis is reversed by omega-3 fatty acid-induced up-regulation of mitofusin 2. Metabolism 2011;60:767–75.
Zhao Y, Joshi-Barve S, Barve S, Chen LH. Eicosapentaenoic acid prevents LPS-induced TNF-alpha expression by preventing NF-kappaB activation. J Am Coll Nutr 2004;23:71–8.
Zhou Y, Zhang X, Chen L, Wu J, Dang H, Wei M, et al. Expression profiling of hepatic genes associated with lipid metabolism in nephritic rats. Am J Physiol Renal Physiol 2008;295:F662–71.